View metadata, citation and similar papers at core.ac.uk
brought to you by CORE
provided by Repositori d'Objectes Digitals per a l'Ensenyament la Recerca i la Cultura

LAPTH-1025/04, IFIC/04-08

Current cosmological bounds on neutrino masses and relativistic relics

Patrick Crotty* and Julien Lesgourgues
Laboratoire de Physique Théorique LAPTH, B.P. 110, F-74941 Annecy-le-Vieux Cedex, France

Sergio Pastor
Instituto de Física Corpuscular (CSIC-Universitat de València), Ed. Institutos de Investigación, Apdo. 22085, E-46071 Valencia, Spain

(Dated: February 4, 2004)

We combine the most recent observations of large-scale structure (2dF and SDSS galaxy surveys) and cosmic microwave anisotropies (WMAP and ACBAR) to put constraints on flat cosmological models where the number of massive neutrinos and of massless relativistic relics are both left arbitrary. We discuss the impact of each dataset and of various priors on our bounds. For the standard case of three thermalized neutrinos, we find $\sum m_\nu < 1.0\,(\text{resp. } 0.6)$ eV (at 2σ), using only CMB and LSS data (resp. including priors from supernovae data and the HST Key Project), a bound that is quite insensitive to the splitting of the total mass between the three species. When the total number of neutrinos or relativistic relics $N_{\rm eff}$ is left free, the upper bound on $\sum m_\nu$ (at 2σ, including all priors) ranges from 1.0 to 1.5 eV depending on the mass splitting. We provide an explanation of the parameter degeneracy that allows larger values of the masses when $N_{\rm eff}$ increases. Finally, we show that the limit on the total neutrino mass is not significantly modified in the presence of primordial gravitational waves, because current data provide a clear distinction between the corresponding effects.

arXiv:hep-ph/0402049v1 5 Feb 2004

I. INTRODUCTION

Neutrino properties are among the most difficult to be probed experimentally, due to the weakness of their interactions. Data from particle accelerators tell us that there are only three flavor neutrinos, while neutrino oscillation experiments show evidence for non-zero neutrino masses (for a recent review, see e.g. [1]). Recent results strongly constrain the mass differences of the individual neutrino masses (actually masses squared, Δm^2) and mixing angles, but no definite conclusion can be drawn neither on the absolute scale of neutrino masses, nor on the existence of weakly coupled sterile neutrinos. Fortunately, cosmology is quite sensitive to the neutrino sector (see [2] for a review), and can shed light on these questions, as well as other interesting issues regarding the Early Universe, such as the process of neutrino decoupling from the primordial plasma.

Currently, the most popular cosmological model is the flat adiabatic ΛCDM scenario, in which the present density of the Universe is shared between baryons, Cold Dark Matter (CDM) and a cosmological constant Λ. This model makes rather simplistic assumptions concerning the neutrino sector, consisting only of three ultra-relativistic neutrinos. It turns out that with a more refined description of the neutrino sector, one finds that only small corrections to the standard picture are allowed after comparing with current data on Cosmic Microwave Background (CMB) anisotropies and Large Scale Structure (LSS). However, these small corrections carry enough interesting physical implications to justify an active research effort, in particular after the first releases of the WMAP and SDSS data. The results of this effort are not only new cosmological bounds on neutrino properties but also a better understanding of how the errors depend on (i) the experimental CMB and LSS data, (ii) external priors on the cosmological parameters, (iii) intrinsic parameter degeneracies in the theory of cosmological perturbations, (iv) assumptions concerning the underlying cosmological model and parameter space.

We here perform a new analysis using the most recent LSS (2dF, SDSS) and CMB (WMAP, ACBAR) data and an extended cosmological model with an arbitrary number of massive neutrinos and additional relativistic particles, parametrized via an effective number of neutrinos ($N_{\rm eff}$). We extend the recent work of [3] and those that appeared after the release of WMAP data [4]-[13]. In particular, our underlying model is identical to that of ref. [13], but our analysis differs since we include an extended set of data (such as the SDSS results and a more updated version of the 2dF ones), a new prior on the matter density from SN-Ia [14] and non-linear corrections to the LSS power spectrum

*Present address: Department of Neurosurgery, University of Virginia Health System, PO Box 800420, Charlottesville, VA 22908, USA

on scales $0.1\,h$ Mpc$^{-1} < k < 0.2\,h$ Mpc^{-1}. Furthermore, we increase the number of free parameters to ten, in order to analyze the bounds in the presence of primordial tensor perturbations.

The rest of the paper is organized as follows. After a short summary of the effects of neutrino masses and additional relativistic particles in Sec. II, we describe our analysis method and dataset in Sec. III. We discuss our results and compare with previous works in Sec. IV. Finally, we conclude in Sec. V.

II. EFFECTS OF ADDITIONAL RELATIVISTIC PARTICLES AND MASSIVE NEUTRINOS

Non-standard neutrinos and other weakly-interacting light particles leave their imprint on the evolution of the Universe, both at the level of background quantities and spatial perturbations. Here we describe the main effects of additional relativistic particles, massive neutrinos and their simultaneous presence.

A. Enhanced relativistic energy density ($N_{\rm eff}$)

The density of radiation in the Universe is usually assumed to be given by that of photons and of three thermally decoupled neutrinos. These contributions are of the same order and fix the evolution of the Universe in the radiation-dominated epoch (RD). Thus, if the three neutrinos did not decouple thermally, or in the presence of sterile neutrinos, the total density of the Universe during RD (as a function of the photon temperature T_γ) would be significantly affected, producing a change in the time of equality between radiation and matter, and in the sound horizon at the time of decoupling. These changes are known to shift the angular scale of the acoustic peaks in the CMB anisotropy spectrum as well as their amplitude (mainly, through the early integrated Sachs-Wolfe effect). They also have an impact on the matter power spectrum $P(k)$, because a shorter matter-dominated stage implies less growth for perturbations inside the Hubble radius. As a consequence, the wave-length corresponding to the maximum in $P(k)$ will be shifted proportionally to the Hubble scale at the time of equality. Thus, the effect of $N_{\rm eff}$ is mainly to change the background evolution. However, ultra-relativistic particles also have a smaller effect directly at the level of perturbations, explained in detail in Ref. [15].

All these effects can be parametrized by a single quantity: the effective number of relativistic degrees of freedom during RD, defined by the relation

$$\rho_r = \left[1 + \frac{7}{8}\left(\frac{4}{11}\right)^{4/3} N_{\rm eff}\right] \frac{\pi^2}{15} T_\gamma^4 \,. \tag{1}$$

Here, ρ_r stands for the total energy density of radiation and $\rho_\gamma = (\pi^2/15)\,T_\gamma^4$ is the contribution of photons. The parameter $N_{\rm eff}$ is defined in such way that if neutrinos decoupled following the instantaneous decoupling approximation, $N_{\rm eff}$ just gives the number of flavor families. However, $N_{\rm eff}$ could differ from three in the presence of extra relics (sterile neutrinos, light gravitons, gravitinos, majorons, effects from extra dimensions, etc.) or in the case of non-thermal decoupling. Actually, in the standard case a careful study of non-instantaneous neutrino decoupling shows that $N_{\rm eff} = 3.04$ for three flavor families [16, 17]. Note that $N_{\rm eff}$ is constant only when the neutrinos or the other relics are ultra-relativistic.

The value of $N_{\rm eff}$ is constrained by Big Bang Nucleosynthesis (BBN) from the comparison with the measured primordial abundances of light elements. During the BBN epoch the nuclear reactions freeze out at a scale factor that depends on the expansion rate, which in turn is fixed by the total energy density of radiation. A BBN analysis shows that $N_{\rm eff} = 2.5^{+1.1}_{-0.9}$ (2σ) [11] (see also [18]), which is perfectly compatible with the number of flavor neutrinos.

However, it is interesting to measure $N_{\rm eff}$ independently of BBN (e.g. using CMB and LSS data) for at least two reasons. First of all, because the number $N_{\rm eff}$ could change between the two epochs [19, 20]. A second reason is because the standard BBN model might be a good first-order description, but with possible corrections due to spatial inhomogeneities, leptonic asymmetries, etc., that could be evaluated with an independent measurement of $N_{\rm eff}$.

B. Massive neutrinos

Neutrinos that possess masses larger or of the same order than the relevant photon temperature have different effects than a constant $N_{\rm eff}$. For instance, neutrinos heavier than roughly 10^{-3} eV are not relativistic today. Neutrino masses have implications for the evolution of cosmological fluctuations, both at the level of background quantities and directly on the perturbations.

It is well-known that massive neutrinos could account for a significant fraction of the total energy density of the Universe today, unlike relativistic thermal relics ($\Omega_r \sim 5.6 \times 10^{-6}$ per neutrino family). For fully non-relativistic flavor neutrinos, the contribution to the present energy density is directly proportional to the number density. For vanishing neutrino chemical potentials, the total neutrino contribution to the critical density is given by

$$\Omega_\nu = \frac{\sum m_\nu}{93.2 \text{ eV}} h^{-2} \ , \tag{2}$$

where h is the Hubble constant in units of 100 km s^{-1} Mpc^{-1} and $\sum m_\nu$ runs over all neutrino mass states. For fixed neutrino masses, Ω_ν would be enhanced if neutrinos decoupled with a significant dimensionless chemical potential $\xi_\nu \equiv \mu_\nu/T$ (or equivalently, for large relic neutrino asymmetries), simply because their number density would increase. In principle there exist some combinations of pairs $(\xi(\nu_e), \xi(\nu_{\mu,\tau}))$ that pass the BBN test and are not yet ruled out by the CMB+LSS limits on $N_{\rm eff}$ [21]. However, it was recently shown that the stringent BBN bounds on ξ_e apply to all flavors, since flavor neutrino oscillations lead to flavor equilibrium before BBN [22, 23, 24]. The contribution of a potential relic neutrino asymmetry is limited to such low values that it can be safely ignored.

When the density of the other fluids (photons, CDM, baryons, dark energy) is kept fixed, the sum over the neutrino masses $\sum m_\nu$ has a direct repercussion on the geometry of the Universe. If instead the spatial curvature is kept fixed, the total mass affects the relative contribution Ω_X of the other fluids. In any case, this background effect has an impact on the observable CMB and LSS power spectra. For masses of the order of 1 eV, this signature is rather small, but can be marginally detectable.

In general, neutrinos tend to stream freely across gravitational potential wells, and to erase density perturbations. Free-streaming is efficient on a characteristic scale called the Jeans length, corresponding roughly to the distance on which neutrinos can travel in a Hubble time. For ultra-relativistic neutrinos, the Jeans length is by definition equal to the Hubble radius c/H, but for non-relativistic ones it grows at a slower rate than c/H (in comoving coordinates, it even decreases with time during matter domination). Neutrinos with masses smaller than approximately $T_{\rm dec} \sim 0.3$ eV are still relativistic at the time of last scattering, and their direct effect on the CMB perturbations is identical to that of massless neutrinos. For bigger masses, the decrease of the free-streaming scale is felt by perturbations which enter inside the Hubble radius before decoupling, which results in a small enhancement of the acoustic peaks with respect to the massless situation.

In the intermediate mass range from 10^{-3} eV to 0.3 eV, the transition to the non-relativistic regime takes place during structure formation, and the matter power spectrum will be directly affected in a mass-dependent way. Wavelengths smaller than the current value of the neutrino Jeans length are suppressed by free-streaming. The largest observable wavelengths, which remain always larger than the neutrino Jeans length, are not affected. Finally, there is a range of intermediate wavelengths which become smaller than the neutrino Jeans length for some time, and then encompass it again: these scales smoothly interpolate between the two regimes. The net signature in the matter power spectrum is a damping of all wavelengths smaller than the Hubble scale at the time of the transition of neutrinos to a non-relativistic regime [25]

$$k > k_{\rm nr} = 0.026 \left(\frac{m_\nu \, \Omega_m}{1 \text{ eV}}\right)^{1/2} h \text{ Mpc}^{-1}. \tag{3}$$

where Ω_m is the contribution of matter to the critical density. The damping is maximal for wavenumbers bigger than the current free-streaming wavenumber $k_{\rm FS}$

$$k > k_{\rm FS} = 0.63 \left(\frac{m_\nu}{1 \text{ eV}}\right) h \text{ Mpc}^{-1}. \tag{4}$$

We have summarized both the background and the direct effects of the neutrino masses on the CMB and LSS perturbations. The total signature is difficult to describe analytically. However, one should remember that for masses of order 1 eV or less, the dominant effect is the one induced by free-streaming on the matter power spectrum. Therefore, the usual strategy is to combine CMB and LSS measurements, where the former roughly fix most of the cosmological parameters, while the latter is sensitive to $k_{\rm FS}$ and provides bounds on the neutrino mass.

C. Combined effects

In a situation with N thermalized massive neutrino species, the cosmological model should include an equal number of parameters, namely $(m_1, \ldots, m_N)$. However, at first order such a model could be described by only two parameters, N and the sum of all individual masses $\sum_{i=1,N} m_i$. This choice not only simplifies the problem, but also provides

the correct contribution of neutrinos to the total energy density both at early times, when all neutrinos are ultra-relativistic and the radiation density depends only on N, and at a late epoch when at least one neutrino mass is large compared with the temperature and the density is given in good approximation by the total mass.

However, for a precise description N and $\sum_{i=1,N} m_i$ are not the only relevant parameters. As an example, let us compare two scenarios with three neutrinos but different mass spectra: a degenerate case with (m_0, m_0, m_0) and a case with $(3m_0, \epsilon, \epsilon)$, where $\epsilon \ll m_0$. In both scenarios the neutrino density is the same for early and late stages of the Universe. But at intermediate temperatures of the order $m_0 \lesssim T_\nu \lesssim 3\, m_0$, the energy densities are different. It is easy to show that the expansion rate is temporarily enhanced in the second scenario, but this will only have a small signature in the CMB spectrum for $m_0 \gtrsim 0.2$ eV. On the other hand, the free-streaming wavenumber $k_{\rm FS}$ of the heaviest neutrino is larger in the second scenario. Thus, in principle we expect more damping and sharper bounds on the mass in the degenerate case.

Nowadays, after many years of experimental effort, we know that neutrinos must be massive in order to explain the evidences for flavor oscillations from measurements of atmospheric and solar neutrinos, independently confirmed by data from the detection of neutrinos from artificial sources at experiments such as K2K and Kamland. These results lead to specific differences between the individual neutrino masses, at two different scales: $\Delta m^2_{\rm atm} \simeq 2.5 \times 10^{-3}$ eV^2 and $\Delta m^2_{\rm sun} \simeq 7 \times 10^{-5}$ eV^2 [1]. But one of the masses remains unconstrained, which reflects the fact that oscillation experiments can not fix the absolute scale of neutrino masses. It is clear that, considering the present cosmological data, in order to have a measurable effect the three neutrinos should have roughly the same mass, following a degenerate scheme (m_0, m_0, m_0), where $m_0 \gtrsim 0.2$ eV.

On the other hand, the positive results from the LSND experiment point to neutrino oscillations with $\Delta m^2 \sim \mathcal{O}(1\ {\rm eV}^2)$. The less disfavored scenario that could explain the LSND data, together with the results of atmospheric and solar neutrino experiments, contains 4 neutrinos following a 3+1 scheme where one of them is much heavier than the others (see for instance [26]) and the fourth neutrino must be sterile. It has been shown [27, 28] that all four neutrino models lead to a full thermalization of the sterile neutrino before BBN, so they are disfavored by BBN. However, current CMB and LSS data can not completely rule out this possibility [7, 13].

The most general scenario is that of a cosmological model with $N^{\rm nr}$ thermally-decoupled massive neutrinos and extra relativistic degrees of freedom, parametrized by $N^{\rm r}$ not necessarily integer. This model is described by a set of $N^{\rm nr}+1$ parameters: $(m_1, \ldots, m_{N^{\rm nr}}, N^{\rm r})$. However, since such a parameter space is too large for a systematic analysis we will consider restricted cases described by only two parameters: the total effective neutrino number $N_{\rm eff} = N^{\rm r} + N^{\rm nr}$ and the total mass M. In order to check the impact of the distribution of the total neutrino mass among the individual states, we will study two cases:

- the model that we call *degenerate* has $N_{\rm eff}$ massive neutrinos with the same mass. Let us emphasize that this is a simplified model where the physical interpretation of non-integer values of $N_{\rm eff}$ is not obvious.
- a second model the we denote *1+r* has only one neutrino with a significant mass, while the other $N_{\rm eff} - 1$ species are ultra-relativistic.

These two models are not chosen arbitrarily. First, the *degenerate* model includes the standard situation with only 3 flavor neutrinos degenerate in mass, while the *1+r* model includes the 3+1 scenario described above. Second, and most importantly, the *degenerate* and *1+r* models appear as limiting situations of the general case once the parameters $N_{\rm eff}$ and M have been fixed. Indeed, the former has the smallest possible value of the free-streaming wavenumber, while the latter has the biggest $k_{\rm FS}$. For any intermediate model (like, for instance, the third case studied in [13], with three effectively massless standard neutrinos and $N_{\rm eff} - 3$ species with equal mass), the observational bounds deduced from the CMB and LSS observations should lay between those that we get in the *degenerate* and *1+r* limits.

III. METHOD AND DATA USED

The WMAP spectrum and many other cosmological data can be accurately fitted with a six-parameter flat ΛCDM model [4, 12], described by the Hubble parameter h, the fractional density of matter $\Omega_m = 1 - \Omega_\Lambda$, the baryon density in dimensionless units $\omega_b = \Omega_b h^2$, the optical depth to reionization τ, and finally, the amplitude and the spectral tilt of primordial perturbations (A_s, n_s). Most of our calculations correspond to a model with eight parameters: the six previous ones plus $N_{\rm eff}$ and M, as previously defined for the *degenerate* and *1+r* models. We will also study the consequences of the presence of a background of primordial gravitational waves, which would contribute to the CMB anisotropy spectrum. For this case, our parameter space will be ten-dimensional, adding the tensor-to-scalar ratio r and the tensor tilt n_t. In all cases, we use the CMBFAST code [29] to calculate the power spectra.

In order to compare the theoretical cosmological models with current observations, we use a Bayesian grid-based method described in some previous works (e.g. [5]), instead of the widely used Monte Carlo Markov Chains (MCMC)

technique employed for instance in [12, 30]. The former has the inconvenient of being considerably slower from the computational point of view, and the advantage of being very robust if the hypersurfaces with the same likelihood in parameter space have very complicated shapes (for instance, an elongated and curved *banana* shape). Also, the MCMC method cannot deal with likelihood distributions with nearly degenerate local minima; mathematically, the existence of local minima cannot be disproved, but in practice, using current data and the wide variety of models discussed in the literature, such a situation never appeared. In order to analyze unusual models with many parameters, it is safe to use at least once a grid-based method, avoiding surprises that could arise from parameter degeneracies. However, our analysis always shows quasi-ellipsoidal likelihood contours for various combinations of parameters. Thus we believe that a MCMC method would give similar results.

For each combination of data set and priors, we plot the Bayesian likelihood of each point in the two-dimensional space of neutrino parameters $(M, N_{\rm eff})$ after marginalization over the other free parameters. Actually, for simplicity we approximate the integration process required for a true marginalization by a maximization of the likelihood over the remaining parameter space. Integration and maximization are known to be equivalent in the case of a multigaussian likelihood distribution and we expect the maximization technique to be reasonably accurate in our case, where we obtained quasi-ellipsoidal contours. We checked this explicitly by computing the marginalized likelihood of each of the six ΛCDM parameters: our results are very close to those of [4, 12], obtained with a MCMC technique and marginalized by integration over the likelihood. Of course, our maximization routine needs to compute the likelihood not only at grid points, but also in between. At a given point in parameter space, this is done by interpolating quadratically each value of the C_l and $P(k)$ from the nearest neighbors of the grid.

Our CMB data include the 1348 correlated points of the Wilkinson Microwave Anisotropy Probe (WMAP), which measure the temperature × temperature (TT) [31] and temperature × E-polarization (TE) [32] correlation functions on the CMB sky. WMAP provides the best available data on multipoles $l \leq 900$. For constraining the TT spectrum on smaller scales, we employ the results of the Arcminute Cosmology Bolometer Array Receiver (ACBAR) experiment [33, 34]. We remove the highest band powers (probing the region $l > 1800$) which could be contaminated by foregrounds. The published ACBAR band powers are decorrelated, so it is self-consistent to use only the first 11 points of data.

Our LSS data set consists of 32 correlated points from the 2 degree Field (2dF) galaxy redshift survey [35], covering the range $0.02\,h\ {\rm Mpc}^{-1} < k < 0.15\,h\ {\rm Mpc}^{-1}$, and of 19 decorrelated points from the Sloan Digital Sky Survey (SDSS) [36] in the range $0.015\,h\ {\rm Mpc}^{-1} < k < 0.20\,h\ {\rm Mpc}^{-1}$. In order to compare the smallest wavelengths with the data, it is necessary to take into account small deviations with respect to the linear power spectrum. Following the analysis in [12], we compute non-linear corrections for each point in parameter space using the numerical procedure described in Appendix C of [37]. Since these corrections rely on N-body simulations of a pure CDM Universe they might not be perfectly optimized for hot plus cold dark matter. However, the models studied here include only a small fraction of non-relativistic neutrino density. Therefore, at first order the fitting formula of [37] should be reasonably accurate in our case (and certainly better than introducing no corrections at all). Each redshift survey is expected to constrain the total matter power spectrum modulo a global normalization factor called the bias b. Unless otherwise stated, all our results were obtained after marginalizing over the 2dF and SDSS bias, treated like two free parameters.

We will also use a prior on the current value of the Hubble parameter, measured by the Hubble Space Telescope (HST) Key project [38]: $h = 0.72 \pm 0.08$ (1σ). Finally, we will impose some constraints on the current density of the cosmological constant deduced from the redshift dependence of type Ia supernovae luminosity. For a flat universe, Perlmutter et al. [39] give a conservative bound $\Omega_m = 0.28 \pm 0.14$ (1σ) that we denote as the SN99 prior. In addition, we will calculate the impact of using the more restrictive result $\Omega_m = 0.28 \pm 0.05$ (1σ) from the recent work by Tonry et al. [14], that we label the SN03 prior.

IV. RESULTS AND COMPARISON WITH PREVIOUS WORKS

A. Degeneracies and priors

In order to understand the impact of each data set and prior on the final results, we will introduce them step by step in the calculation of the likelihood. We will first focus on the *degenerate* model.

We start using only CMB and LSS data without any prior, apart from the top-hat priors defined implicitly by the boundaries of our grid. We look for the two-dimensional probability distribution of the neutrino parameters in the range $0 < M < 2.25\,{\rm eV}$ and $1 < N_{\rm eff} < 9$. We find that most of this parameter space is allowed at 2σ, as shown in panel (a) of Fig. 1. Actually some of the grid boundaries are reached by the allowed models [55], unlike in the rest of our analysis where they have no influence on the 2σ allowed regions.

The physical explanation for such loose constraints is well-known: when the density of relativistic relics is left free,

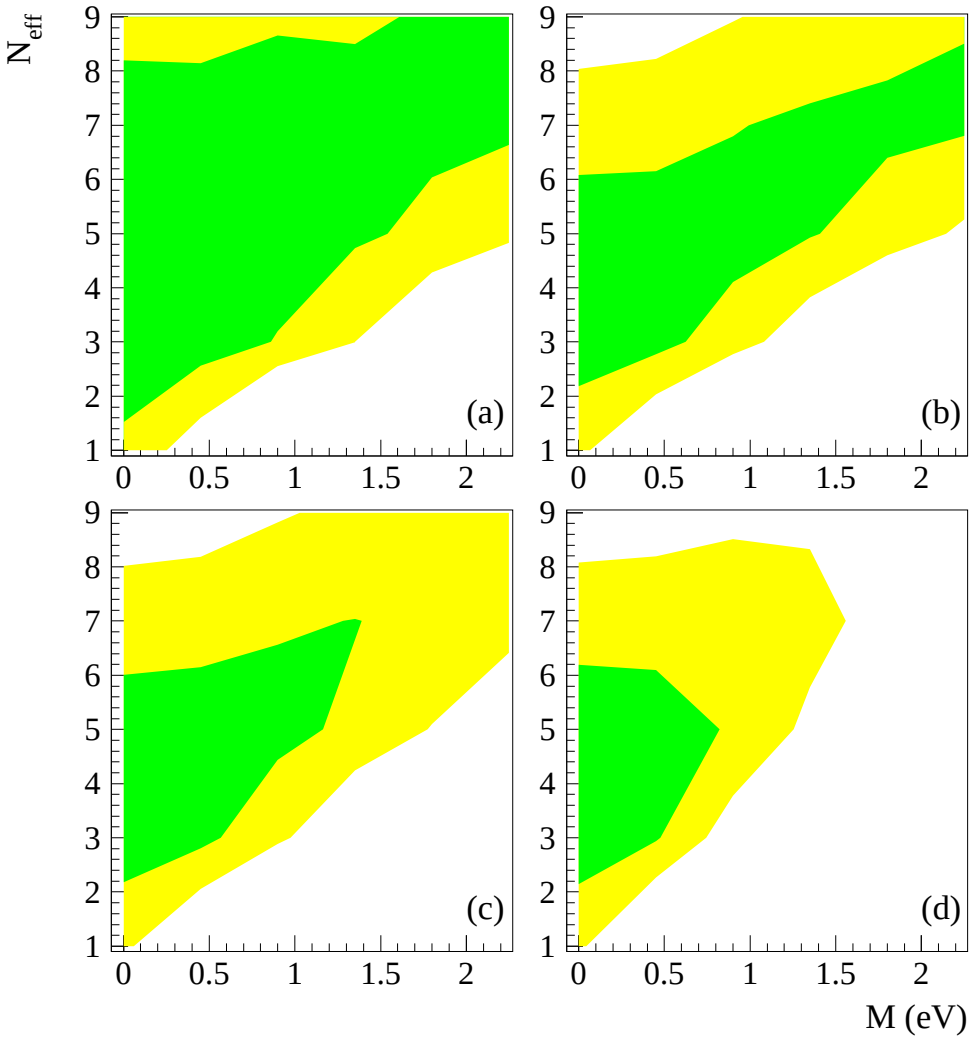

FIG. 1: Two-dimensional likelihood in $(N_{\rm eff}, M)$ space, marginalized over the six remaining parameters of the model. We plot the 1σ (green / dark) and 2σ (yellow / light) allowed regions. Here we used CMB (WMAP & ACBAR) and LSS (2dF & SDSS) data, adding different external priors as defined in section III: (a) no priors, (b) HST, (c) HST+SN99, (d) HST+SN03.

there is a parameter degeneracy between

$$\omega_r \equiv \Omega_r h^2 = 2.47 \times 10^{-5}\, h^2 \left(\frac{T_{\rm CMB}}{2.725\,{\rm K}}\right)^4 \left[1 + \frac{7}{8}\left(\frac{4}{11}\right)^{4/3} N_{\rm eff}\right] \tag{5}$$

and $\omega_m \equiv \Omega_m h^2$. Indeed, one can vary these two quantities in the same proportion while keeping fixed $z_{\rm eq}$, the redshift of equality between matter and radiation. In order to remove this degeneracy, it is necessary to impose some priors on h and Ω_m. Thus we repeat the same analysis, using now the HST prior. In this case, we obtain a band of allowed models shown in panel (b) of Fig. 1. This region stretches up to the maximal values of M and $N_{\rm eff}$ in our grid, so we cannot derive yet limits on these parameters. However, the other grid bounds are now irrelevant, since none of the models allowed at 2σ ever reaches them. The 1σ preferred region includes models with $(M = 0,\ N_{\rm eff} = 3.04)$, showing that there is no evidence for massive neutrinos and/or extra relativistic degrees of freedom. However, it is interesting to see that large departures from the standard ΛCDM model cannot be excluded.

These results show clearly how difficult is to put bounds on the neutrino mass in presence of an excess of relativistic relics during RD, and vice versa. For instance, if we assume $N_{\rm eff} = 3$, we get a 2σ upper bound $M < 0.8$ eV, while for $N_{\rm eff} = 6$ this bound spectacularly increases to $M < 2.2$ eV. This trend was already observed in [7, 8, 13, 40], and can be explained as follows. Suppose that we start from the best-fit standard model with $(M = 0,\ N_{\rm eff} = 3)$, and

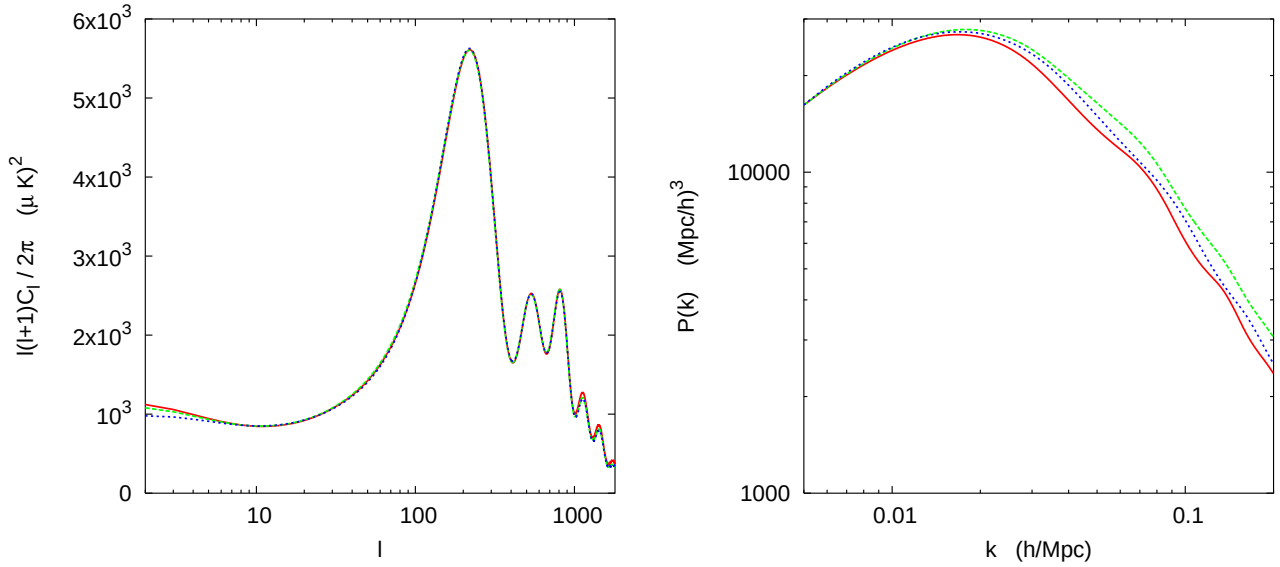

FIG. 2: Illustration of the main parameter degeneracy affecting our results. For three particular models, we plot on the left the CMB temperature spectrum (normalized to WMAP) and on the right the matter power spectrum (two of them have been rescaled by hand for clarity). See the main text for details.

that we increase $N_{\rm eff}$ in such way that the radiation density in the early Universe is multiplied by a factor α. Then, in order to keep the CMB power spectra roughly constant, we should maintain a fixed value both for $z_{\rm eq}$ and Ω_Λ. This would be achieved with a transformation of the type $(\omega_m, h) \longrightarrow (\alpha\,\omega_m, \sqrt{\alpha}\,h)$. However, it is well-known that the shape of the matter power spectrum is given roughly by the parameter $\Gamma = \Omega_m h$, that scales like $\sqrt{\alpha}\,\Gamma$ with the previous transformation, meaning that the spectrum will have more power on small scales relatively to large scales. A neutrino mass can balance this increase through the free-streaming effect. Therefore, models with high values of $N_{\rm eff}$ are compatible with larger neutrino masses.

We illustrate this parameter degeneracy in Fig. 2, where we show the CMB temperature spectrum (normalized to WMAP) and the matter power spectrum for three particular models. The first model (red/solid curves) is the best-fit model for the standard case $(M, N_{\rm eff}) = (0, 3)$. In the second model (green/dashed curves), we have increased the number of degrees of freedom to $N_{\rm eff} = 7$ and performed the transformation on $(\omega_m,\, h)$ as previously discussed, leaving both z_{eq} and Ω_M invariant. We have also increased n_s a little bit. On the CMB figure it is difficult to distinguish the curves because they perfectly overlap, especially for the best measured scales (those of the first acoustic peak), while the difference at $l < 10$ is masked by cosmic variance. But as expected, the shape of the matter power spectrum is modified, with more power on small scales relatively to large scales. This leaves plenty of room for models with a significant neutrino mass and free-streaming effect, like the one featured here (blue/dotted curve) which has $(M, N_{\rm eff}) = (2.25\,{\rm eV}, 7)$.

In order to obtain bounds on the mass, it is necessary to add more restrictive priors. In particular, the supernova priors should help to better constrain Ω_m (around the central value 0.28) and therefore also the shape parameter Γ (around $\Omega_m h = 0.28 \times 0.72 = 0.20$). This value of Γ is in very good agreement with the constraint obtained from LSS data, assuming no neutrino mass: the SDSS power spectrum points to $\Gamma = 0.21 \pm 0.03$ [36]. Therefore, we expect the SN prior to restrict the possibility of a large neutrino free-streaming effect and to improve the upper bound on M. This is what we observe by successively adding the SN99 and SN03 priors in our analysis. The corresponding contours, shown in panels (c) and (d) of Fig. 1, are the main results of this work. With the SN03 prior, our one-dimensional bounds on the effective neutrino number (marginalized over M) read $1.6 < N_{\rm eff} < 7.2$ at 2σ, in very good agreement with our previous results $1.4 < N_{\rm eff} < 6.8$ [5] obtained without SDSS, no SN priors and fixing $M = 0$. The one-dimensional upper bound on the total neutrino mass (marginalized over $N_{\rm eff}$) is $M < 1.1$ eV at 2σ. For comparison, we list the bounds for fixed integer values of $N_{\rm eff}$ are in Table I, for different priors. Since we use more recent 2dF and SDSS data, as well as more restrictive SN priors, we are not surprised to find stronger bounds than Hannestad & Raffelt [13].

	degenerate		1+r	
$N_{\rm eff}$	no priors	HST+SN03	no priors	HST+SN03
3	1.0	0.6	0.8	0.6
4	1.5	0.8	1.2	0.8
5	2.0	1.0	1.6	1.1
6	–	1.1	1.9	1.4
7	–	1.0	–	1.5

TABLE I: The 2σ upper bound on the total neutrino mass M (eV), after marginalization over the six cosmological parameters of the flat ΛCDM model, for particular values of $N_{\rm eff}$. We show the results for two limiting cases of splitting the total mass between the neutrino states: *degenerate* (all neutrinos with the same mass) and *1+r* (one massive neutrino and the other treated as relativistic relics). Here we have used the full CMB and LSS data set, either alone (no priors) or combined with the HST and SN03 priors. For large $N_{\rm eff}$ values and in absence of priors, the upper bound is larger than the maximal value of M in our grid (2.25 eV).

B. Role of LSS data

So far we have used the LSS data as an indication of the shape of the matter power spectrum, but not its overall amplitude. This amplitude is difficult to measure, because of possible differences between the two-point correlation function of luminous galaxies and that of matter, a problem known as the bias uncertainty. The 2dF team has established that the bias b is almost scale-independent, and derived some constraints either on the redshift distortion parameter $\beta = \Omega_m^{0.6}/b$ [41] or directly on b [42]. These two results must be employed with great care since the bias is expected to depend on the mean luminosity and redshift of each particular galaxy sample. In order to use a self-consistent bias prior, we would need to compute some correction factors for each model (see for instance refs. [8, 30, 43]). This technically difficult procedure, that relies on many assumptions, is beyond the goal of the present paper and we prefer to conservatively discard any bias prior, as in [12]. Just for indication, we tried to repeat the previous analysis with a very naive bias prior. Instead of leaving the 2dF bias as a free parameter, we tried to add the constraint $\Omega_m^{0.6}/b_{\rm 2dF} = 0.43 \pm 0.07$ [41] to our full set of data and priors (which includes all the CMB+LSS data, the HST prior, and one of our two supernovae priors). As shown in panel (a) of Fig. 3, our results remain unchanged. This is consistent with the analysis of Elgarøy & Lahav [8], who treat the bias prior in a detailed way and find no impact on the neutrino mass determination.

Since the LSS data plays a crucial role in constraining the neutrino mass, it is worth comparing the impact of the 2dF and SDSS power spectra. We go back to a data set consisting of CMB+LSS+HST+SN99, and remove either the SDSS or 2dF spectrum from the analysis. The results, shown in panels (b) and (c) of Fig. 3, should be compared with the combined analysis previously shown in (c) of Fig. 1. The SDSS power spectrum appears to be much more conservative, in good agreement with previous papers: the WMAP+SDSS constraint on the neutrino mass for $N_{\rm eff} = 3$ is as large as $M < 1.74$ eV [12], while a WMAP+other CMB+2dF analysis gives $M < 0.69$ eV [4]. Consistently, our combined analysis gives intermediate results: for $N_{\rm eff} = 3$ our WMAP+ACBAR+2dF+SDSS bound is $M < 0.9$ eV. Our results seem also consistent with the recent analysis in [3], where the corresponding bound $M < 0.75$ eV was found including data from both galaxy surveys up to $k \lesssim 0.15\,h$ Mpc^{-1}.

Note that in order to employ the SDSS data until $k_{\rm max} \simeq 0.20\,h$ Mpc^{-1}, it is crucial to include the non-linear corrections to the matter power spectrum, in particular for the $N_{\rm eff}$ bounds. The panel (d) of Fig. 1 was obtained with all the CMB and LSS data, plus the HST and SN99 priors, but in absence of non-linear corrections. A comparison with Fig. 1c shows that the constraints on $N_{\rm eff}$ are lifted by one unit. This can be easily understood. Fig. 4 shows a typical power spectrum with and without non-linear corrections. The linear power spectrum has less power on small scales, i.e. a smaller effective shape parameter Γ. As explained earlier in this section, this can be easily compensated by an appropriate increase in $N_{\rm eff}$, ω_m and h, while leaving the CMB spectrum almost invariant.

C. Adding tensors

We have discussed so far the dependence of our results under the choice of data set and priors. However, generally speaking, the bounds on a particular parameter also depend on assumptions concerning the underlying cosmological model, a simple six-parameter flat ΛCDM model in our case. It is clear that by adding extra physical ingredients that would compensate the effect of neutrinos, we would relax the bounds on ($N_{\rm eff}$, M). It is inviable to perform a systematic study of all the ΛCDM variants proposed in the literature, but one of them deserves a particular interest. Indeed, the six-parameter ΛCDM relies on the existence of super-horizon cosmological fluctuations at early times,

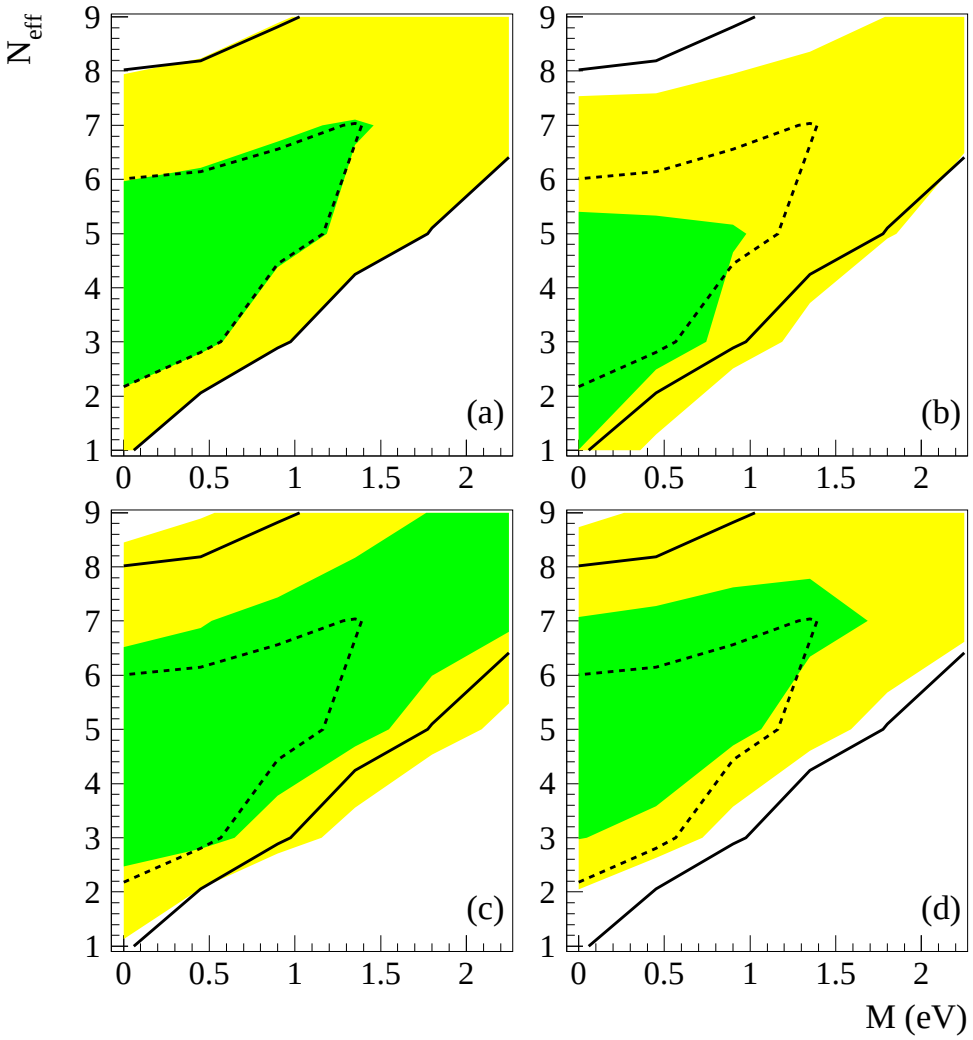

FIG. 3: Impact of various assumptions related to the LSS data set. The default model for which we show 1σ (dashed) and 2σ (solid) contours was obtained with WMAP, ACBAR, 2dF, SDSS, plus the HST and SN99 priors. Each panel shows the 1σ (green / dark) and 2σ (yellow / light) allowed regions (a) when including the 2dF bias prior [41], (b) without the SDSS data, (c) without the 2dF data, (d) without non-linear corrections.

which strongly suggests that perturbations are of inflationary origin. But inflation also predicts a background of primordial tensor perturbations: the question is whether these gravitational waves are large enough to contribute to large-scale CMB anisotropies (fundamentally, this depends on the energy scale of inflation). It is thus important to see how the neutrino parameter bounds evolve in presence of two extra parameters, the relative amplitude and tilt of the primordial tensor spectrum (r, n_t).

Previous analyses [4, 12] showed that for eight-parameter models (flat ΛCDM + tensors) a significant contribution of gravitational waves is disfavored. However, one could expect that in a ten-dimensional model (flat ΛCDM + tensors, with $N_{\rm eff}$ and M), a new parameter degeneracy would show up and relax the various bounds. We performed such an analysis for our full CMB and LSS data set, adding the HST and SN03 priors. The resulting two-dimensional likelihood for ($N_{\rm eff}$, M), marginalized over the other eight parameters, is shown in Fig. 5. It is almost indistinguishable from that with a vanishing contribution of gravitational waves, which shows that the current data is clearly able to distinguish between the respective effects of tensors and neutrinos. Thus the cosmological bound on neutrino masses is robust with respect to tensors. This robustness also holds when including a non-adiabatic, incoherent contribution to the power spectrum such as those predicted by topological defects, as shown in a very recent work [44].

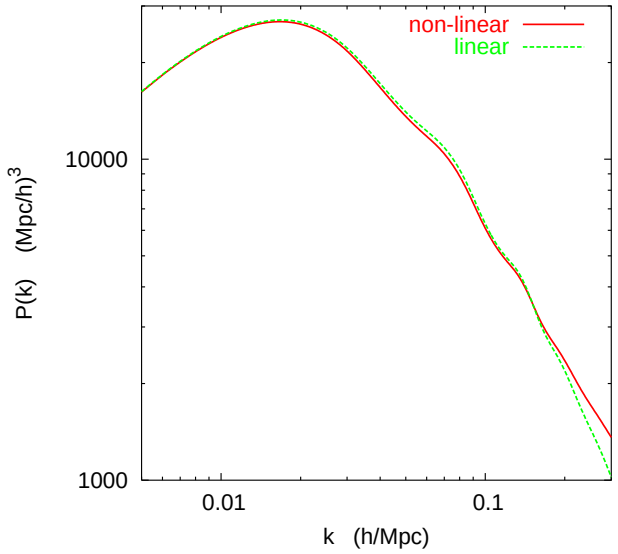

FIG. 4: Matter power spectrum for the best-fit model with $(M, N_{\rm eff}) = (0, 3)$, plotted with and without non-linear corrections. The difference becomes significant in the region $k > 0.15\,h$ Mpc^{-1} probed by the last two points in the SDSS data set.

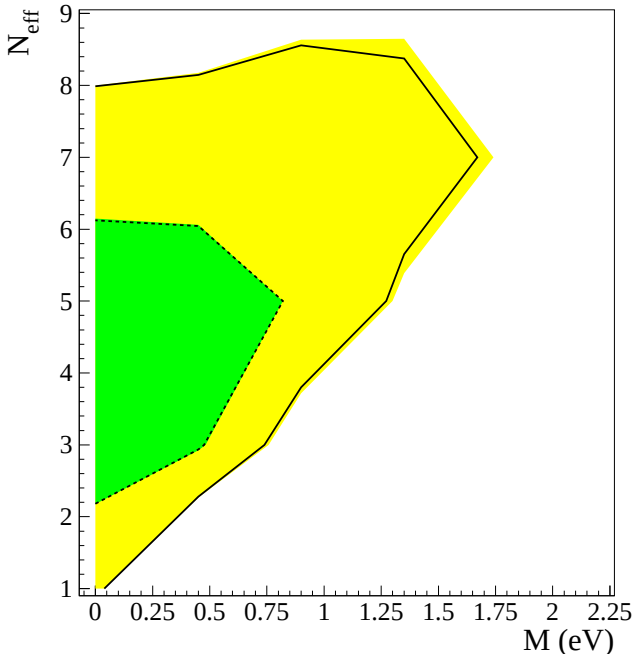

FIG. 5: 1σ (green / dark) and 2σ (yellow / light) allowed regions in (M, $N_{\rm eff}$) space, marginalized over the eight other free parameters of the flat ΛCDM+tensors model. For comparison, we show the contours corresponding to the case with no gravitational waves. The difference is very small, showing the ability of the data to make a clear difference between the effect of neutrinos and gravitational waves.

D. Impact of mass splitting

Our aim is to constrain cosmological models with an arbitrary number of massive neutrinos and with extra relativistic degrees of freedom. However, so far we reduced the analysis to two parameters (M, $N_{\rm eff}$), with the implicit assumption that all neutrinos were degenerate in mass. We have not discussed the fact that for a fixed total number of degrees of freedom $N_{\rm eff}$ and total mass M, the evolution of cosmological perturbations depends on the splitting of the mass between the different species.

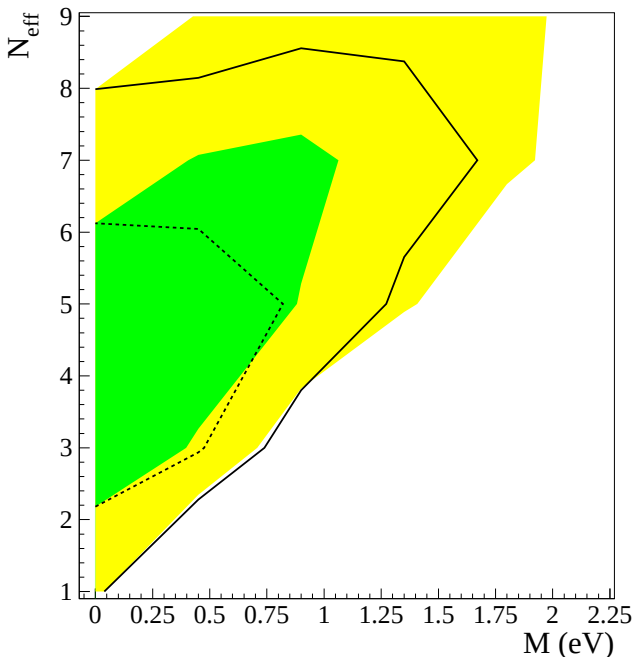

FIG. 6: 1σ (green / dark) and 2σ (yellow / light) allowed regions in (M, $N_{\rm eff}$) space for the *1+r* model, compared with the *degenerate* model (dashed 1σ and solid 2σ contours). Here we have included all CMB and LSS data, plus the HST and SN03 priors.

As explained in section II, for fixed (M, $N_{\rm eff}$), in some sense the opposite case to the *degenerate* model is the *1+r* scenario, for which all the mass corresponds to a single neutrino eigenstate, instead of being equally shared. We built a second grid of *1+r* models and analyzed it with our most restrictive set of data (WMAP+ACBAR+2dF+SDSS) and priors (HST+SN03). We show in Fig. 6 the new allowed regions, compared with the previous ones. In the limit of small mass and small $N_{\rm eff}$, the CMB and LSS power spectra are almost identical in the two cases, because the effect of the mass splitting is second-order with respect to that of the total mass. A priori, this does not guarantee that the (M, $N_{\rm eff}$) iso-likelihood contours are asymptotically equal, because we are doing a Bayesian analysis and the contours are defined with respect to the best-fit model. For instance, in Ref. [13], the best-fit models for the *degenerate* and *1+r* cases correspond to high values of (M, $N_{\rm eff}$) and are different from each other. This explains why the authors find different contours in the two cases even in the massless limit. The same occurs in our analysis when we do not impose any prior. However, when at least the HST prior is taken into account, the best-fit model is very close to $(M, N_{\rm eff}) = (0, 3)$ and the contours only differ at high values of M and $N_{\rm eff}$. As expected from the physical discussion in Sec. II, the model with only one massive neutrino is less constrained: remember that in that case, for a fixed M the free-streaming wavenumber $k_{\rm FS}$ is larger. Therefore, the damping of the matter power spectrum is less efficient. The one-dimensional bounds on the effective number of neutrinos (marginalized over M) now reads $1.6 < N_{\rm eff} < 8.5$ at 2σ, and the limit on the total neutrino mass (marginalized over $N_{\rm eff}$) increases to $M < 1.5$ eV (2σ). The bounds for fixed integer values of $N_{\rm eff}$ are given in the last column of Table I.

V. CONCLUSIONS

We have calculated cosmological bounds on neutrino masses and relativistic relics ($N_{\rm eff}$) using the latest data on CMB (WMAP and ACBAR) and LSS (SDSS and 2dF galaxy surveys) in the framework of an extended flat ΛCDM. In the cases in which a comparison is possible, our results are in good agreement with those of previous analyses [3]-[13]. In the well motivated case of three flavor neutrino with degenerate masses, we found an upper limit on the total masses of $M < 1.0$ (resp. 0.6) eV using only CMB and LSS data and priors (resp. including priors on h and Ω_Λ). The bound for four thermalized neutrinos with only one of them carrying a significant mass is $M < 0.8 - 1.2$ eV, depending on the priors used. Therefore, the 4-neutrino solution to the LSND results is not completely ruled out, but some tension with cosmological data exists, especially if the strong SN03 prior is taken into account.

In the case of arbitrary $N_{\rm eff}$, our results are summarized in Fig. 1 and listed in Table I. They clearly show the

existence of a parameter degeneracy between the total neutrino mass and $N_{\rm eff}$, a trend already observed in previous works [7, 8, 13, 40] that we have explained in Sec. IV. External priors on h and Ω_Λ are found to be of particular importance for constraining respectively $N_{\rm eff}$ and M.

Since the standard ΛCDM model (with its three effectively massless thermal relics) sits within the 1σ preferred region, we find no evidence for exotic physics such as out-of-equilibrium neutrino decoupling, non-standard nucleosynthesis, extra relativistic relics, a significant amount of hot dark matter, etc. However, large deviations from the standard case are still compatible with observations: for instance, a model with one neutrino of mass $M = 1.5$ eV and eight relativistic degrees of freedom is allowed by CMB and LSS data, even when all priors are included (see Fig. 6). In order to exclude this model, it is necessary to take into account the prediction of standard BBN, which gives stronger limits on $N_{\rm eff}$.

The bounds obtained in this paper are based on the observation of cosmological perturbations (CMB and LSS), combined with constraints on the current expansion and acceleration rates of the Universe (HST and SN priors). Therefore they are completely independent from the predictions of primordial nucleosynthesis. It is remarkable that in the space of the two standard BBN free parameters $(\omega_b, N_{\rm eff})$, the preferred regions deduced from cosmological perturbations and from primordial abundances are perfectly compatible with each other, and more or less orthogonal: indeed, our analysis (with the most restrictive priors) gives $0.0215 < \omega_b < 0.0235$ and $1.6 < N_{\rm eff} < 8.5$, while standard BBN favors $0.017 < \omega_b < 0.026$ and $1.6 < N_{\rm eff} < 3.6$ [11] (all these bounds are at the 2σ level).

In order to test their robustness, we have also calculated the bounds on M and $N_{\rm eff}$ in the presence of primordial tensor perturbations. Our results show that the bounds are practically unchanged, because current cosmological data is able to distinguish between the respective effects of tensors and neutrinos.

Finally, we have considered the impact of a different splitting of the total neutrino mass among the individual states, an analysis also recently performed in ref. [13]. We compared the case of complete mass degeneracy (all neutrinos with the same mass) with that where one neutrino state effectively possesses the whole mass. We found that the bounds on the degenerate case are more restrictive due to its more efficient free-streaming, in particular for larger values if $N_{\rm eff}$. However, for three or four neutrinos the differences between the two cases are not significant.

Our bounds are a clear indication that present cosmological data provide interesting bounds on the neutrino sector, complementary to those from terrestrial experiments. These include tritium beta decay experiments, which provide a current upper bound on the total neutrino mass of 6.6 eV at 2σ [45], while the KATRIN experiment [46] is planned to have an accuracy of the order 0.35 eV. Sub-eV sensitivity to neutrino masses is also expected for experiments measuring neutrinoless double beta decays [47], but only for Majorana neutrinos and with a dependence on the details of the mixing matrix.

However, the cosmological bounds should be taken with care, due to their dependence on the data (or priors) used, and also on the assumption of a particular underlying model. Examples are given by the works [10, 48], where non-zero neutrino masses are preferred. This warning should not prevent us to be confident on the power of future cosmological experiments to limit (and eventually detect) neutrino masses and other neutrino properties. For instance, forecast analyses have shown that with future data there will be potential sensitivities to $\Delta N_{\rm eff} \sim 0.2$ [15, 49] (eventually improving BBN results) and neutrino masses of the order $0.1 - 0.2$ eV with Planck and final SDSS data [50, 51, 52], or with galaxy and CMB lensing [53, 54].

Acknowledgments

This research was supported by a CICYT-IN2P3 agreement. SP was supported by the Spanish grant BFM2002-00345, the ESF network Neutrino Astrophysics and a Ramón y Cajal contract of MCyT.

[1] M. Maltoni, talk given at AHEP-2003, Valencia (Spain), Oct 2003 [hep-ph/0401042].
[2] A.D. Dolgov, Phys. Rept. **370**, 333 (2002) [hep-ph/0202122].
[3] V. Barger, D. Marfatia and A. Tregre, hep-ph/0312065.
[4] D.N. Spergel et al., Astrophys. J. Suppl. **148**, 175 (2003) [astro-ph/0302209].
[5] P. Crotty, J. Lesgourgues and S. Pastor, Phys. Rev. D **67**, 123005 (2003) [astro-ph/0302337].
[6] E. Pierpaoli, Mon. Not. Roy. Astron. Soc. **342**, L63 (2003) [astro-ph/0302465].
[7] S. Hannestad, JCAP **0305**, 004 (2003) [astro-ph/0303076].
[8] Ø. Elgarøy and O. Lahav, JCAP **0304**, 004 (2003) [astro-ph/0303089].
[9] V. Barger, J.P. Kneller, H.S. Lee, D. Marfatia and G. Steigman, Phys. Lett. B **566**, 8 (2003) [hep-ph/0305075].
[10] S.W. Allen, R.W. Schmidt and S.L. Bridle, Mon. Not. Roy. Astron. Soc. **346**, 593 (2003) [astro-ph/0306386].
[11] A. Cuoco, F. Iocco, G. Mangano, G. Miele, O. Pisanti and P.D. Serpico, astro-ph/0307213.

[12] M. Tegmark et al. [SDSS Coll.], astro-ph/0310723.
[13] S. Hannestad and G. Raffelt, hep-ph/0312154.
[14] J.L. Tonry et al., Astrophys. J. **594**, 1 (2003) [astro-ph/0305008].
[15] S. Bashinsky and U. Seljak, astro-ph/0310198.
[16] A.D. Dolgov, S.H. Hansen and D.V. Semikoz, Nucl. Phys. B **503**, 426 (1997) [hep-ph/9703315].
[17] G. Mangano, G. Miele, S. Pastor and M. Peloso, Phys. Lett. B **534**, 8 (2002) [astro-ph/0111408].
[18] R.H. Cyburt, B.D. Fields and K.A. Olive, Phys. Lett. B **567**, 227 (2003) [astro-ph/0302431].
[19] M.J. White, G. Gelmini and J. Silk, Phys. Rev. D **51**, 2669 (1995) [astro-ph/9411098].
[20] M. Kaplinghat and M.S. Turner, Phys. Rev. Lett. **86**, 385 (2001) [astro-ph/0007454].
[21] J. Lesgourgues and S. Pastor, Phys. Rev. D **60**, 103521 (1999) [hep-ph/9904411].
[22] A.D. Dolgov et al., Nucl. Phys. B **632**, 363 (2002) [hep-ph/0201287].
[23] Y.Y. Wong, Phys. Rev. D **66**, 025015 (2002) [hep-ph/0203180].
[24] K.N. Abazajian, J.F. Beacom and N.F. Bell, Phys. Rev. D **66**, 013008 (2002) [astro-ph/0203442].
[25] W. Hu, D.J. Eisenstein and M. Tegmark, Phys. Rev. Lett. **80**, 5255 (1998) [astro-ph/9712057].
[26] T. Schwetz, talk given at AHEP-2003, Valencia (Spain), Oct 2003 [hep-ph/0311217].
[27] P. Di Bari, Phys. Rev. D **65**, 043509 (2002). [hep-ph/0108182].
[28] K.N. Abazajian, Astropart. Phys. **19**, 303 (2003) [astro-ph/0205238].
[29] U. Seljak and M. Zaldarriaga, Astrophys. J. **469**, 437 (1996) [astro-ph/9603033].
[30] L. Verde et al., Astrophys. J. Suppl. **148**, 195 (2003) [astro-ph/0302218].
[31] G. Hinshaw et al., Astrophys. J. Suppl. **148**, 135 (2003) [astro-ph/0302217].
[32] A. Kogut et al., Astrophys. J. Suppl. **148**, 161 (2003) [astro-ph/0302213].
[33] C. Kuo et al. [ACBAR Coll.], Astrophys. J. **600**, 32 (2004) [astro-ph/0212289].
[34] J.H. Goldstein et al., Astrophys. J. **599**, 773 (2003) [astro-ph/0212517].
[35] W.J. Percival et al., Mon. Not. Roy. Astron. Soc. **327**, 1297 (2001) [astro-ph/0105252].
[36] M. Tegmark et al. [SDSS Coll.], astro-ph/0310725.
[37] R.E. Smith et al. [The Virgo Consortium Coll.], Mon. Not. Roy. Astron. Soc. **341**, 1311 (2003) [astro-ph/0207664].
[38] W.L. Freedman et al., Astrophys. J. **553**, 47 (2001) [astro-ph/0012376].
[39] S. Perlmutter et al. [Supernova Cosmology Project Coll.], Astrophys. J. **517**, 565 (1999) [astro-ph/9812133].
[40] J. Lesgourgues and A.R. Liddle, Mon. Not. Roy. Astron. Soc. **327**, 1307 (2001) [astro-ph/0105361].
[41] J.A. Peacock et al., Nature **410**, 169 (2001) [astro-ph/0103143].
[42] L. Verde et al., Mon. Not. Roy. Astron. Soc. **335** (2002) 432 [astro-ph/0112161].
[43] O. Lahav et al., astro-ph/0112162.
[44] R.H. Brandenberger, A. Mazumdar and M. Yamaguchi, hep-ph/0401239.
[45] J. Bonn et al., Nucl. Phys. Proc. Suppl. **91**, 273 (2001).
[46] A. Osipowicz et al. [KATRIN Coll.], hep-ex/0109033.
[47] S.R. Elliott and P. Vogel, Ann. Rev. Nucl. Part. Sci. **52**, 115 (2002) [hep-ph/0202264].
[48] A. Blanchard, M. Douspis, M. Rowan-Robinson and S. Sarkar, Astron. Astrophys. **412**, 35 (2003) [astro-ph/0304237].
[49] R. Bowen et al., Mon. Not. Roy. Astron. Soc. **334**, 760 (2002) [astro-ph/0110636].
[50] D.J. Eisenstein, W. Hu and M. Tegmark, Astrophys. J. **518**, 2 (1998) [astro-ph/9807130].
[51] J. Lesgourgues, S. Pastor and S. Prunet, Phys. Rev. D **62**, 023001 (2000) [hep-ph/9912363].
[52] S. Hannestad, Phys. Rev. D **67**, 085017 (2003) [astro-ph/0211106].
[53] M. Kaplinghat, L. Knox and Y.S. Song, astro-ph/0303344.
[54] K.N. Abazajian and S. Dodelson, Phys. Rev. Lett. **91**, 041301 (2003) [astro-ph/0212216].
[55] For fixed $N_{\rm eff} < 2$ or $N_{\rm eff} > 8$, the best-fit models reach the extreme values of $h \in [0.58, 0.90]$ and $\omega_m \in [0.11, 0.25]$. However, the global maximum-likelihood fit has $(M, N_{\rm eff}) = (0, 3)$ and values of the other cosmological parameters well inside the grid boundaries.